DIFFUSION COEFFICIENT MEASUREMENT BY HIGH RESOLUTION NMR SPECTROSCOPY: BIOCHEMICAL AND PHARMACEUTICAL APPLICATIONS

John C. Lindon[1*], Maili Liu[2] and Jeremy K. Nicholson[1]

[1]*Biological Chemistry, Biomedical Sciences Division, Imperial College of Science, Technology and Medicine, Sir Alexander Fleming Building, South Kensington, London SW7 2AZ UK.*

[2]*Laboratory of Magnetic Resonance and Atomic and Molecular Physics, Wuhan Institute of Physics and Mathematics, The Chinese Academy of Sciences, Wuhan 430071, P.R. China.*

CONTENTS

Page

Summary 24
1. Introduction 24
2. High resolution NMR diffusion coefficient measurement methods 25
   2.1 The Stimulated Echo Method (STE) 25
   2.2 The Longitudinal-Eddy-Current Delay (LED) method 26
   2.3 Use of Heteronuclear NMR 29
   2.4 The LED sequence combined with 2-dimensional NMR 30
   2.5 Artifacts 31
3. Applications of NMR diffusion measurements 32
   3.1. Editing complex spectra of mixtures 32
   3.2. Measurement of diffusion coefficients in biofluids 36
   3.3. Drug-protein binding 41
   3.4. Impurity characterization in pharmaceuticals 50
   3.5. Solvent accessibility of protein and peptide NH groups 55
4. References 62

*To whom correspondence should addressed.
Tel +44-(171)-594-3194; Fax +44-(171)-594-3066; Email j.lindon@ic.ac.uk

SUMMARY

Recently there has been renewed interest in the measurement of molecular diffusion coefficients using NMR spectroscopy, building on the pioneering experiments of thirty years ago. This has arisen because of the development of new NMR hardware and pulse sequences, which allow the diffusion coefficients relating to individual peaks in a high resolution NMR spectrum to be determined. In our laboratories we have been applying this approach to provide improved characterization of individual molecules in complex mixtures such as biofluids and to measure diffusion coefficients in such mixtures to investigate molecular dynamics and interactions. We have also used the approach to edit NMR spectra of mixtures on the basis of molecular size and thus to characterize monomeric and dimeric species in pharmaceutical materials. We have also been using the measurement of diffusion coefficients to study molecular interactions such as drug-protein binding and the lifetimes of NH protons in peptides and proteins as a measure of their solvent accessibility thus giving information of secondary structure. These recent results are summarized, together with the pertinent experimental details.

1. INTRODUCTION

Originally, molecular diffusion coefficients were measured by the pulsed-field-gradient spin-echo (PFG-SE) NMR spectroscopic method and this approach has been reviewed by Stilbs.[1] The measurement of diffusion coefficients using NMR spectroscopy can be traced back to the experiments of Stejksal and Tanner in 1965.[2] They first showed that in a spin-echo (SE) NMR experiment, the use of a pulsed magnetic field gradient (PFG) to provide spatial labeling followed by a period to allow diffusion and then a second, rephasing, gradient could give information on how far a molecule had moved in the diffusion period. A typical PFG-SE pulse sequence is 90° -G-180°-G-FID, where G represents a pulsed magnetic field gradient, and NMR signal attenuation is given by,

$$A(g) = A(0) \exp[(\gamma g)^2 D(\Delta-\delta/3)-2t_s/T_2] \quad (1)$$

Here A(g) and A(0) are the signal intensities in the presence and absence of the PFG pulse, γ is the gyromagnetic ratio of the spin, g and δ are the strength and duration of the rectangular gradient, Δ is the time between the starting point of the two gradients, D is the diffusion coefficient of the molecule, t_s is the total spin-echo time and T_2 is the transverse relaxation time. The main problem with the use of field gradient pulses in high resolution NMR spectrometers is the field distortion caused by eddy currents generated in the metal components of the NMR probe which arise from switching of the gradient pulses. This has largely been overcome by the use of pulse sequences that compensate for eddy currents and the use of shielded gradient coils. More recently, the ability to apply magnetic field gradient pulses on high resolution NMR spectrometers has opened up the field such that almost any modern high resolution NMR spectrometer is capable of carrying out such studies.

2. HIGH RESOLUTION NMR DIFFUSION COEFFICIENT MEASUREMENT METHODS

2.1 The stimulated-echo method (STE)

The STE pulse sequence for diffusion coefficient measurement comprises three 90° pulses that can result an in echo after the third pulse.[3-5] The echo was named by Hahn[3] the "stimulated echo", which is unique in that its relaxation attenuation has a T_1 dependence during the interval between the second and third 90° pulses, whereas the normal spin-echo (SE) attenuates according to T_2 as the period after the initial pulse is increased (see Equation 1). The use of the STE in NMR diffusion measurement had been described in detail by Tanner[4] and the methods for elimination of unwanted echoes and reduction of dead time in STE experiment had been investigated.[5] The advantages of using the pulsed-field gradient stimulated-echo method (PFG-STE) for diffusion coefficient measurement are that, for systems, where $T_1 > T_2$ and low diffusion coefficient, it is possible to use longer diffusion times to achieve measurable attenuation and in the situation where the diffusion coefficients depend on the diffusion time (such as in restricted diffusion), it is possible to extend the diffusion times to the maximum without phase distortion caused by J-coupling.

Apart from the difference in the relaxation attenuation, another difference between the PFG-SE and PFG-STE methods is the coherence transfer pathways. In the PFG-SE experiment, the diffusion occurs in a single quantum (SQ) state and there is no coherence transfer process after the SQ is generated by the 90° pulse. However, in the PFG-STE experiment, the SQ exists between the first and second RF pulses and after the third RF pulse. The SQ coherence is converted to zero quantum (ZQ) during the free diffusion period (t_d) and the two gradient pulses ($G_{1,2}$) serve as both diffusion and coherence selection gradients. If the two PFG pulses are identical (with the same strengths and duration) in the PFG-STE experiment, the observed signal is given by:

$$A(g) = ½\, A(0) \exp[-(\gamma g \delta)^2 D(\Delta - \delta/3) - 2t_s/T_2 - t_d/T_1] \quad (2)$$

The definitions of the parameters in Equation 2 are the same as in Equation 1 with the exception that t_s is the time interval between the first and second RF pulses or the time between the third RF pulse and the start of data acquisition, t_d is the free diffusion time between the second and third RF pulse. The constant ½ is a reduction factor as a result of using PFGs for coherence selection.

2.2 The Longitudinal-Eddy-Current-Delay (LED) Method

Diffusion coefficient measurement experiments have become much more widely applied following the developments of self-shielded PFG probes and advanced NMR pulse sequences, such as the longitudinal-eddy-current-delay (LED) sequence (Figure 1(a)).[6] These techniques can greatly reduce the eddy-current effects induced by the PFG pulses. The LED sequence is a modification of the PFG-STE experiment by introducing a second ZQ delay (filter) period to allow any possible eddy-currents to decay away before data acquisition. This is achieved by placing the magnetization during the diffusion period back along the z-axis and hence the method is named the longitudinal eddy-current delay.[6]

A modified LED sequence incorporating bipolar-gradient pulses as this further reduces eddy current effects has also been published,[7] in which a 180° RF pulse sandwiched by two PFG pulses with opposed polarities (i.e. bipolar), is used to replace the single gradient pulse. There are two advantages of using bipolar gradients. Firstly, the eddy-currents and the effect

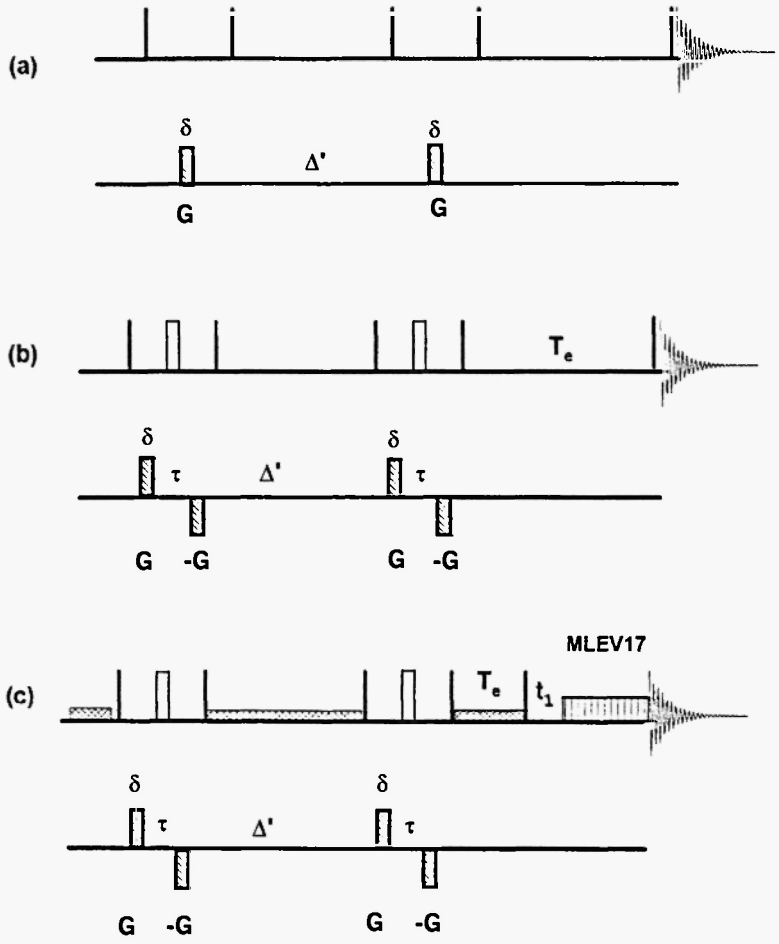

Fig. 1: Pulse sequences for editing ^{1}H NMR spectra on the basis of molecular diffusion. (a) The basic LED method with pulse field gradients. (b) Incorporating bipolar gradients and editing on the basis of differences in diffusion coefficients and T_2 relaxation times, the DIRE sequence. (c) The pulse sequence for the measurement of diffusion coefficients using ^{1}H-^{1}H DETOCSY NMR spectra employing the MLEV-17 spin lock method with water resonance suppression. The hatched areas indicate the periods for which saturation of the water resonance was applied. δ is the duration of the pulsed field gradient G (which can be rectangular or be shaped to avoid fast rise and fall times), τ is the time between bipolar gradients, Δ' is the diffusion period, T_e is a gradient recovery delay and t_1 is the two-dimensional increment time. The narrow bars are 90° pulses, the open rectangles are 180° pulses, and details of the cycling of the phases of the RF pulses have been given earlier.[25]

of the gradient pulses on the lock signal are reduced to a minimum since the two bipolar pulses are placed very close in time. Secondly, the action of the bipolar pulses is the same for the diffusion measurement and coherence selection as in the LED sequence, but the effective gradient output is doubled. This should be useful for the systems with low diffusion coefficients where large gradients are needed.

In addition, it is now possible to shape the gradient pulses to avoid the artefacts caused by the very fast rise and fall times of rectangular gradients. Shaped gradients are usually Gaussian or sine-shaped. The diffusion coefficients can be obtained by fitting the intensity of the NMR resonances as a function of the square of the applied gradient strength according to Equation (3)

$$A(g) = \tfrac{1}{2} A(0) \exp[-(S\gamma g\delta)^2 D(\Delta - \delta/3 - \tau/2) - 2t_s/T_2 - t_d/T_1] \quad (3)$$

where S is a gradient shape factor ($S = 2/\pi$ for a sine-shaped gradient, and $S = \omega_{1/2}/8$ for a Gaussian-shaped gradient, where $\omega_{1/2}$ is the half line-width of the Gaussian shape) and τ is the time interval between the bipolar gradients.

It is now usual to fix the time intervals and vary the gradient strength outputs for diffusion coefficient measurement. In this case the attenuation caused by the relaxation (both T_1 and T_2) is constant throughout the experiments and the equation can be shortened to

$$A(g) = A(0) \exp(-K'D). \quad (4)$$

where K' is an attenuation factor relating to the PFGs. Thus $K' = (\gamma g\delta)^2 D(\Delta - \delta/3)$ for the SE, STE and LED methods and $K' = (S\gamma g\delta)^2 D(\Delta - \delta/3 - \tau/2)$ for the bipolar-LED method, and the reduction due to relaxation is included in A(0).

When the results are plotted as a contour plot in a pseudo-two-dimensional display with NMR chemical shifts on the horizontal axis and the derived diffusion coefficients on the vertical axis, the method has been termed diffusion-ordered spectroscopy (DOSY).[8] Recently, DOSY and diffusion coefficient measurement in general has been used to probe vesicle size distributions in phospholipids,[9] combinatorial chemistry libraries,[10-12] macrocycle-cyclodextrin complexes,[13] the trapping of small molecules in vesicles,[14] polymer molecular weight distributions,[15] analysis of a complex mixture from a cell extract,[16] protein-protein association,[17,18] protein-ligand

interactions,[19,20] protein unfolding,[21] insulin aggregation,[22] albumin-SDS interactions,[23] ion-pair aggregation,[24] and characterization of biofluids.[25,26]

It is well known that it is possible to edit ^{1}H NMR spectra according to the T_1 and T_2 relaxation times of the nuclei. However, it is also possible to take advantage of NMR resonance intensity attenuation caused by the application of magnetic field gradients and a pulse sequence which provides spectral editing based on differences in diffusion coefficients as well as relaxation is given in Figure 1(b). This can be combined with various solvent resonance suppression schemes and this allowed the experiments to be carried out on aqueous solutions. In addition, we also used sine-shaped bipolar gradients to minimize spectral artefacts.[25] In one implementation, the usual 180° refocusing RF pulse was replaced by a "3-9-19-19-9-3" pulse train which is the same as that used in the WATERGATE sequence for solvent resonance elimination.[27] Since the "3-9-19-19-9-3" pulse train has no effect on the on-resonance solvent magnetization and is equivalent to a 180° pulse for the off-resonance magnetization, the bipolar gradient labels the spatial positions only of the off-resonance spins. The detection part starts with another spin-echo scheme in which another pair of bipolar gradients with identical strength and duration is used for refocussing and the spin-echo time is kept minimal. A zero quantum filter with a delay of 50 ms, together with a fifth gradient was inserted before data acquisition to remove the phase distortion caused by spin-spin couplings and to further reduce the eddy current artifact induced by the use of gradients.

2.3 Use of Heteronuclear NMR

It has been demonstrated that it is feasible to use heteronuclear NMR detection for the measurement of diffusion coefficients, in particular ^{13}C NMR spectroscopy.[28]

The use of measured diffusion coefficients to study ligand-protein binding has been described by Lennon *et al.*[29] who used the resolved ^{31}P NMR resonances of 2,3-diphosphoglycerate to study its interaction with haemoglobin inside red blood cells. They have also taken into account effects of differing T_2 values of the free and bound ligand in cases where this would result in different proportions of the free and bound ligand being "NMR-invisible".[30]

Recently, we have shown that if diffusion is allowed to occur during a pulse sequence in which the gradients are applied during a period of multiple quantum (MQ) coherence, then their effect is increased by a factor equal to the coherence level and this then allows smaller gradient strengths to be used and still have the same dephasing and rephasing effects. This could be important for slowly diffusing molecules where small field gradients have little effect on NMR signal intensities.[31]

There are two advantages in using the heteronuclear multiple coherence for diffusion coefficient measurement. Firstly, the use of MQ coherence can greatly enhance the diffusion attenuation and thus it is possible to achieve a larger dynamic range of attenuation with less gradient strength output, which should be useful for reducing the eddy-current effect and for working with slowly diffusing systems. Secondly, detection in the heteronuclear domain can reduce the problems of signal overlap or background peaks, and solvent resonance suppression (for biological systems). Although, the low natural abundance of some nuclei (^{13}C, ^{15}N, etc) will cause problems of sensitivity, the use of ^{19}F and ^{31}P NMR respectively is expected to be widely exploited for diffusion studies of drugs and energy related phosphates in biological systems.

2.4 The LED Sequence Combined with 2-Dimensional NMR

Incorporation of the "diffusion ordered spectroscopy" (DOSY) approach to 2-dimensional NMR spectra has been achieved using DOSY-NOESY on a nucleotide[32] and using COSY-DOSY on a mixture of three amino acids in D_2O[33] and the idea of combining 2-dimensional NMR with diffusion measurement in other pulse sequences has been suggested.[33] The implementation of a DOSY-HMQC experiment using ^{1}H-^{13}C correlation has also been reported.[34,35] The use of DOSY-NOESY and DOSY-HMQC methods have practical difficulties for diffusion coefficient measurement because the generally small NOEs are limited to a few internuclear pairs and the low natural abundance and inherent insensitivity of ^{13}C produce NMR spectra with rather low signal-noise ratios and this makes quantitative determination of diffusion coefficients difficult. In addition, the magnitude or phase-alternating line shape of the DOSY-COSY experiment limits its application for quantitative work. On the other hand the ^{1}H-^{1}H total correlation NMR method, TOCSY, is more suitable for diffusion coefficient measurement because of the high signal-noise ratios easily achieved, the large

number of cross peak resonances giving replicated information and the absorptive in-phase line shape. TOCSY-DOSY experiments have been reported on human blood plasma,[25] on a mixture of alcohols[34] and also on a mixture of polypropylene and decane.[36] We have termed the experiment diffusion-edited TOCSY or DETOCSY and the pulse sequence is shown in Figure 1(c).[25]

2.5 Artifacts

The major problems associated with NMR diffusion measurement include eddy currents, thermal gradient convection and the effects of spin-spin coupling. Eddy currents are induced in the metal parts of the NMR probe by the fast rise and fall times of electric currents in the gradient coil. These in turn induce an oscillating voltage in the detector coil. The use of self-compensated power supplies and the design of self-shielded gradient coil probes can effectively minimize the eddy currents and the application of bipolar PFGs can further improve the eddy-current suppression efficiency.

Thermal convection is associated with the temperature control of the NMR tube. Most NMR spectrometers use a stream of temperature-regulated gas (nitrogen or air) to control the sample temperature. The gas is commonly fed back into the probe through the bottom of probe. When the temperature of the gas is above room temperature, a temperature gradient results along the sample tube. If the thermal gradients are large enough, convective flow can occur in the NMR tube.[37] In addition, the switching of gradient pulses with their consequential heating effects can cause time-dependent temperature gradients. Convection had been noted and analyzed by Carr and Purcell[38] in very early NMR studies of diffusion. They had indicated that if convection current exits, the second echo is larger than the first echo in a multiple gradient spin-echo experiment. The mathematical explanation of the effect and a simple method to remove the convection effect is to measure the even number echo instead of the odd number echo.[38] A similar idea has been applied in the LED and bipolar-LED methods by doubling the pulse sequences.[39,40] It has also been reported that the convection can be effectively eliminated by rotating the sample.[41] Unfortunately, such an approach is unsuitable for diffusion coefficient measurement. Other solutions proposed for overcoming the effects of convection caused by thermal gradients include the use of a liquid thermal bath around the NMR tube[42] or the application of

pulse field gradients using either x-axis or y-axis gradient coils since most thermal convection lies along the tube axis (z-axis).

A number of data processing methods have been used to improve the determination of diffusion coefficients from DOSY NMR spectra and these include the application of maximum entropy[43] and multivariate curve resolution[44] methods.

3. APPLICATIONS OF NMR DIFFUSION COEFFICIENT MEASUREMENTS

3.1 Editing complex spectra of mixtures

A major difficulty encountered in NMR spectroscopic studies of complex biological samples such as biofluids arises from the considerable range of concentrations, molecular weights and molecular mobility (hence NMR line width) of the individual organic components. Traditionally, in bioanalysis, such problems have mainly been resolved by extensive sample preparation using physical methods such as chromatographic separations.[45] However, this process may cause both biological and physicochemical property changes of the sample, and hence the measured biochemical composition may differ from that actually occurring in the intact biomatrix. One major advantage of using NMR spectroscopy to study complex biomixtures is that measurements can often be made with minimal sample preparation (usually with only the addition of 5-10% D_2O) and a detailed analytical profile can be obtained on the whole biological sample. To achieve this, it is also necessary to suppress the solvent water resonance and hence much effort has been expended in discovering efficient new NMR pulse sequence techniques for spectral simplification and water suppression and one of the most successful is the WATERGATE method[27] which has been enhanced recently.[46]

The editing of ^{1}H NMR spectra of biofluids based on diffusion alone or on a combination of spin relaxation and diffusion has been presented recently. A new pulse sequence has been reported which combines the effect of molecular diffusion and transverse relaxation times on the spectra of biofluids and also allows the suppression of the solvent water NMR resonance. We have termed this the Diffusion and Relaxation Editing (DIRE) pulse sequence.[25] This approach is complementary to the editing of ^{1}H NMR spectra based on differences in T_1 and T_2 reviewed by Rabenstein *et al.*[47]

One of the major approaches to the assignment of resonances in the NMR

spectra of biofluids relies on the measurement of resonance connectivities using 2-dimensional NMR spectroscopy, particularly COSY[48] and TOCSY.[49] The latter technique has two advantages in that the off-diagonal cross peaks are all in-phase and additional information on spin coupling connectivities along chains of coupled protons is obtained. Even so, 2-dimensional correlation spectra of complex biofluids show much overlap of cross-peaks[50] and further editing is often desirable. New methods for editing TOCSY spectra of biofluids have been given, in this case based on differences in molecular diffusion coefficients and this has been termed Diffusion Edited TOCSY (DETOCSY).[25]

The method has been tested using human blood plasma with 5% D_2O added to provide a field-frequency lock for the NMR measurements. The NMR experiments were carried out at 400 MHz using an instrument with a field gradient accessory capable of delivering a z-field gradient up to 590 $mT.m^{-1}$. Figure 2(a) shows a normal one-pulse ^1H NMR spectrum of control human blood plasma with water suppression. The broad background from albumin and the broad peaks from the lipoproteins are clearly visible as are sharp peaks from a number of small molecule endogenous metabolites. Many of the resonances have been assigned[50] and some key assignments are given on the figure.

The ^1H NMR spectrum of human blood plasma shown in Figure 2(b) was acquired using the pulse sequence given in Figure 1(b). Figure 2(b) was acquired using a relatively strong gradient, of 295 $mT.m^{-1}$, and the resonances from the small molecules are reduced substantially due to their relatively fast diffusion compared to those of the larger molecules that give rise to the broad peaks in the spectrum. The lipoprotein resonances arise from different positions within the fatty acid chains. In addition, the signal from the choline methyl groups of the phospholipid content of the lipoproteins can be seen at δ3.2 now clearly resolved from the resonance of the H2 proton of β-glucose.[50] The relatively sharp peaks near δ2 arise from the *N*-acetyl groups of the carbohydrate component of glycoproteins and their appearance in this edited spectrum confirms that they are from macromolecular systems. Other peaks are observed between δ3.4 and δ3.9 and these have been assigned to the glycerol protons and to the methylene groups of the choline group in phosholipids in lipoproteins based on the measurement of NMR spectra of model compounds. Elimination by diffusion editing of the many resonances which normally occur in this region of the spectrum arising mainly from amino acids and carbohydrates has allowed the observation of these

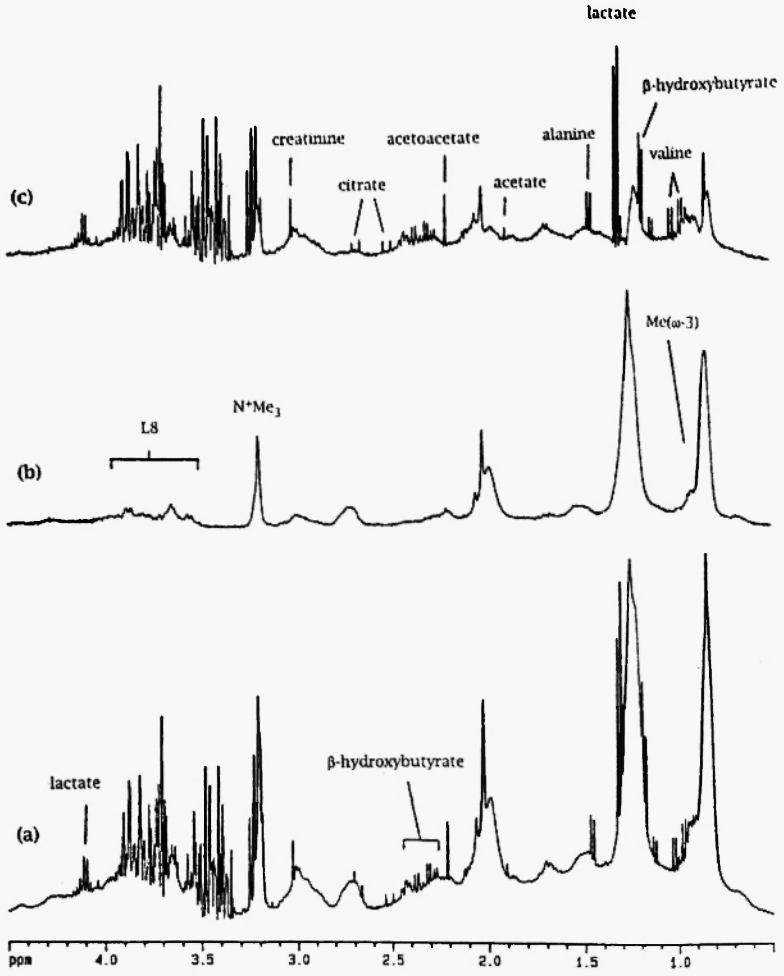

Fig. 2: 400 MHz ^{1}H NMR spectra of control human blood plasma with solvent water elimination and edited on the basis of differences in diffusion coefficients using the pulse sequence of Figure 1(b). (a) normal spectrum, (b) spectrum with gradient application at 295 mT.m^{-1} and (c) the difference between (a) and (b). Assignments - Albumin resonances: A1, A2 - methyl and lysyl ε-CH_2 resonances respectively; lipoprotein resonances: L1 - CH_3; L2 - -$(CH_2)_n$-; L3 - $CH_2.CH_2.CO$; L4 - $CH_2.CH_2.CH$=; L5 - $CH_2.CH$=; L6 - =$CH.CH_2.CH$=; L7 - CH=, L8 - choline and glycerol protons of phospholipids; Region A: amino acids and carbohydrates, mainly α- and β-glucose; N-acetyl: *N*-acetyl resonances from carbohydrate units of glycoproteins, principally $_1$-acid glycoprotein; N^+Me_3 - N-trimethyl group of choline in phospholipids; Me(ω-3) - CH_3 resonance from $CH_3.CH_2.CH$= containing fatty acids in lipoproteins.

phospholipid peaks for the first time in the ^{1}H NMR spectra of intact plasma. Figure 2(c) is the difference between Figure 2(a) and Figure 2(b), where nearly all resonances are from small, fast diffusing molecules and assignments are as shown. Thus this approach provides a simple method to obtain edited NMR spectra of either the large or small molecular weight components. The ability to remove the resonances from the small molecules may be important in view of the increasing number of studies reporting lipoprotein analyses in whole plasma by using line shape fitting algorithms.[51]

It is clear that it is possible to edit NMR spectra of biofluids to remove resonances from small rapidly diffusing molecules using diffusion editing and from rapidly relaxing molecules by relaxation editing. It is possible, in principle, to combine these two approaches in the DIRE pulse sequence such that molecules in a given window of mobility give rise to NMR resonances.

It is possible to monitor the intensity of every data point in an NMR spectrum as a function of the square of the applied field gradient and determine, on the assumption of a single exponential decay, an apparent diffusion coefficient for every data point. If the apparent diffusion coefficient is then plotted as an alternative to the usual spectral intensity, a "diffusion weighted" NMR spectrum results. Unlike the conventional NMR spectrum, the intensities now relate to metabolite molecular diffusion rather than concentration. We have previously demonstrated how NMR-derived metabolite concentrations can be used as input to pattern recognition methods in order to classify biofluid samples in terms of toxic insult[52,53] or disease[54,55] and we have proposed the possibility of using "diffusion weighted" NMR spectra for classifying biofluid samples where the classification will be based on differences in molecular mobility rather than concentration.[25,26] We are currently investigating this possibility.

The approach can also be extended to multidimensional NMR spectroscopy of complex mixtures and the diffusion editing sequence has also been incorporated into the TOCSY pulse sequence with water suppression as shown in Figure 1(c). This results in a total correlation 2-dimensional NMR spectrum in which editing of both diagonal and cross-peaks can be achieved on the basis of the molecular diffusion coefficients. Thus Figure 3 shows a series of TOCSY spectra of control human blood plasma with application of increasing field gradient strengths using the pulse sequence of Figure 1(c) in order to attenuate resonances from faster diffusing molecules. Figure 3(a) shows resonances from both large and small molecules, many of which have been assigned previously.[50] The key assignments are as given in Figure 2.

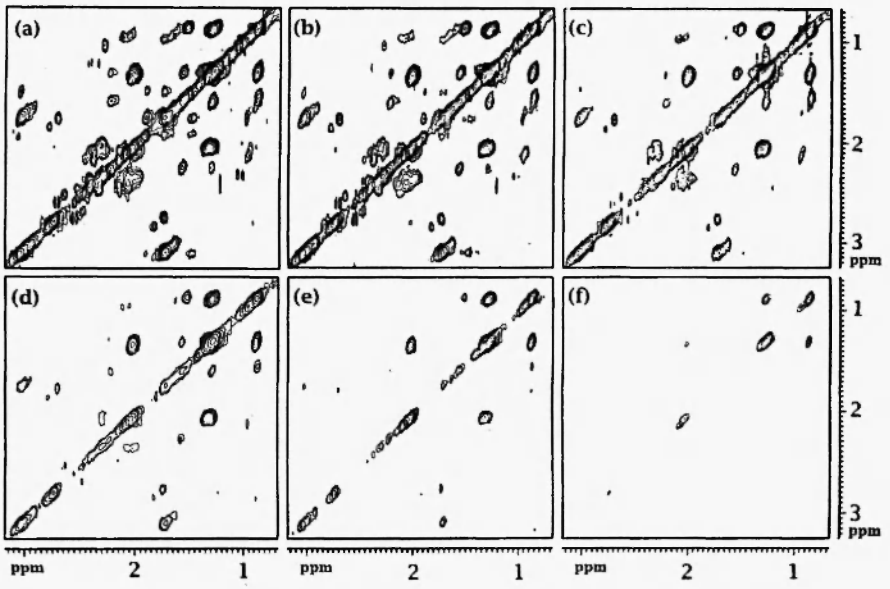

Fig. 3: A series of 600 MHz ^{1}H-^{1}H DETOCSY NMR spectra acquired with a range of gradient strengths using the pulse sequence given in Figure 1(c) illustrating the progressive attenuation of the signal intensities. (a) g = 21.3 mT.m^{-1}, (b) g = 95.8 mT.m^{-1}, (c) g = 170.3 mT.m^{-1}, (d) g = 244.8 mT.m^{-1}, (e) g = 319.3 mT.m^{-1} and (f) g = 393.8 mT.m^{-1}.

However, on application of the DETOCSY pulse sequence, the resonances from the fast-diffusing small molecules are attenuated, leaving principally resonances from the lipoproteins. The assignments of these resonances are given on Figure 2. The coupling connectivities of the resonances from the choline and glycerol protons of phospholipids between δ3.6 and 4.0 can now be analyzed in detail as they are no longer obscured by resonances from small molecules, such as α- and β-glucose and amino acids, which appear in this region.

3.2 Measurement of diffusion coefficients in biofluids

The two-dimensional ^{1}H DETOCSY NMR method described above has been used to measure diffusion coefficients in a biofluid. In addition, it should be noted that diffusion coefficients can be used in an interactive way

with the conventional approach using chemical shifts and coupling constants for NMR resonance assignment in biofluids where there is a large molecular weight range.

These experiments were carried out on a spectrometer operating at 600 MHz for ^{1}H observation on an instrument equipped with a 5 mm triple resonance (^{1}H, ^{13}C, ^{15}N) probe incorporating an actively shielded z-gradient coil. The probe temperature was maintained at 37°C throughout. The pulse sequence used was similar to that given earlier[25] except a saturation approach was used to suppress the water NMR resonance. Eight data sets were acquired under identical conditions except for the gradient strength which was initially set to 21.3 $mT.m^{-1}$ and increased by 74.5 $mT.m^{-1}$ for each successive data set acquired. In order to attain thermal equilibrium for the spin-lock DETOCSY experiment, 128 dummy scans were used prior to data acquisition. The volume integrals of the cross-peaks were used to calculate the diffusion coefficients.

A series of six DETOCSY NMR spectra of human blood plasma are shown in Figure 3. These cover the chemical shift range δ3.1 to δ0.8 with increasing gradient strength, where the cross-peaks from the small and freely-moving molecules are attenuated using a smaller gradient whereas those from the larger components or small molecules which are bound to macromolecules require a larger field gradient to cause attenuation.

An extended region of the 2-dimensional DETOCSY NMR spectrum between δ6.0 - δ0.5 is shown in Figure 4 using only a very low gradient of 21.3 $mT.m^{-1}$ so that this is virtually identical to the normal TOCSY spectrum. The cross-peaks have been numbered and the assignments are shown in Table 1.[50] It can be seen that for most major components there are one or more pairs of cross-peaks for each molecule which are well separated and thus these provide the possibility for measuring diffusion coefficients with more accuracy using a single exponential function. The results of such a fit are listed in Table 1

It can be seen from Table 1 that the measured values of diffusion coefficients fall in a range of approximately 1 10^{-10} m^2s^{-1} to 14 10^{-10} m^2s^{-1} ranging from the macromolecular complexes such as lipoproteins to very small freely diffusing substances such as valine. The various resonances for the residues of albumin yield an average value for the diffusion coefficient of albumin in human blood plasma of about 2 10^{-10} m^2s^{-1}. The diffusion coefficients for the small endogenous species that are not bound to plasma

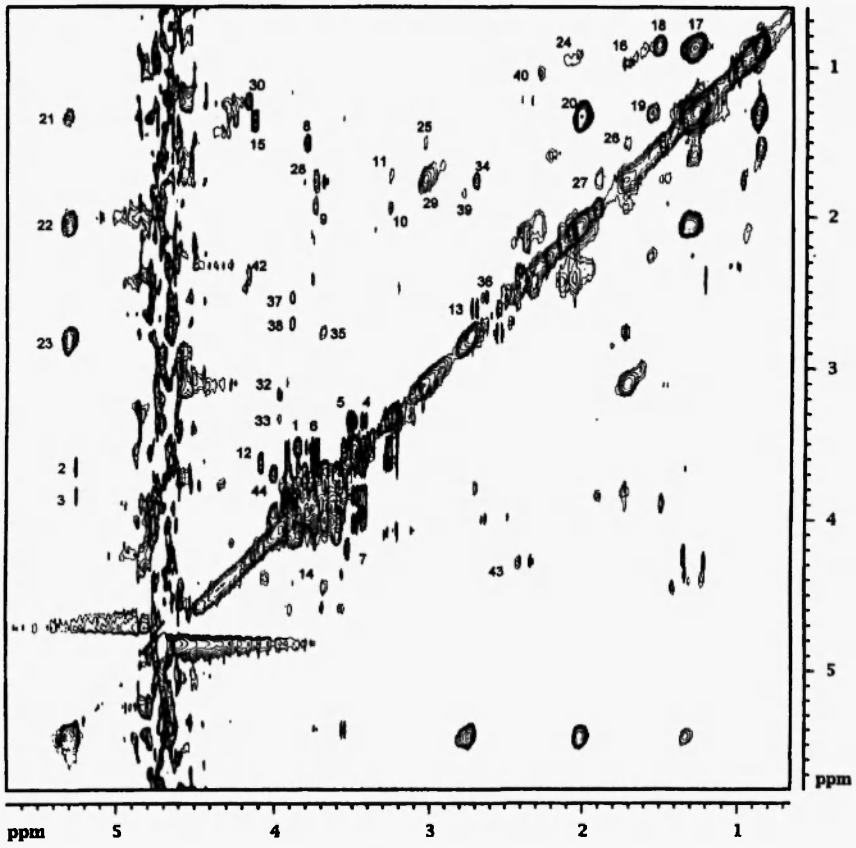

Fig. 4: 600 MHz ^{1}H-^{1}H DETOCSY NMR spectrum of human blood plasma acquired using the pulse sequence in Figure 1, but with a low value of the gradient (21.3 mT.m^{-1}). Each cross peak is numbered and its assignment is given in Table 1.

macromolecules have values as expected based on molecular size. However, other substances show smaller values than would be expected on the basis of their size and this may indicate an interaction with a plasma macromolecule. These include citrate, lysine and threonine.

Diffusion coefficients have also been measured for the various lipoprotein resonances. These are well separated for the various functional groups such as choline glycerophosphoryl moieties and for the different alkyl and alkenyl positions of the fatty acids of the lipids. It was not possible, however, to resolve separate peaks in the 2-dimensional DETOCSY NMR spectra from

Table 1

Diffusion coefficients of endogenous substances in human blood plasma measured from ^1H-^1H 2D-TOCSY NMR cross peak volumes

Peak number	Cross-peak chemical shifts	Assignment	Average D ($\times 10^{-10}$ $m^2.s^{-1}$)
1-3	3.41,3.83; 3.53, 5.22; 3.71,5.23	α-glucose	7.9
4-7	3.24,3.40; 3.24,3.48; 3.43,3.73; 3.46,3.90	β-glucose	7.6
8	1.46,3.78	alanine	12.8
9-11	1.89,3.72; 1.89,3.24; 1.65,3.24	arginine	9.4
12	3.51,4.06	choline	10.5
13	2.52,2.68	citrate	4.8
15	1.32,4.11	lactate	8.2
16	0.90,1.65	leucine	4.4
14,17-23, 39	4.30,3.65; 0.85,1.26; 0.84,1.49; 1.26,1.53; 1.28,1.98; 5.29,1.30; 5.28,1.99; 2.74,5.28; 1.80,2.75	lipoproteins	1.2
24,29,34-37,44	0.92,2.04; 1.46,2.99; 1.71,2.67; 2.67,3.66; 2.44,2.61; 2.45,3.86; 3.57,3.98	HSA	2.1
25,26	1.46,3.01; 1.45,1.69	lysine	4.8
27,28	1.68,1.89; 1.72,3.71	lysine, arginine	5.4
30	1.19,4.14	threonine	4.9
31	6.89,7.18	tyrosine	5.9
32	3.09, 3.94	creatine	12.4
33	3.26, 3.95	betaine	13.9
38	2.62, 3.86	aspartate	8.5
40	1.02, 2.25	valine	12.9
42, 43	2.30, 4.14; 4.15, 2.38	proline	10.2

the different classes of lipoproteins such as LDL, VLDL, IDL and HDL. It is recognized that these particles, having very different molecular sizes, will have different translational diffusion coefficients. However, in this study all gradient strength dependence of the NMR spectral intensities of the lipoprotein cross peaks could be fitted using a single exponential function and this resulted in an average diffusion coefficient of 1.2 10^{-10} m^2s^{-1}. It appears

that a higher NMR magnetic field strength or the use of 1-dimensional NMR with increased digital resolution would be required in order to introduce sufficient increased chemical shift dispersion to allow measurement of diffusion properties of the various lipoproteins.

The benefits in spectral dispersion which result from the use of 2-dimensional NMR methods must be offset against the increased time required to collect the NMR data. Whereas for a diffusion coefficient measurement using 1-dimensional ^{1}H NMR spectroscopy, it is possible to collect NMR spectra for each of the required 10-16 gradient values in a few minutes, the corresponding time for 2-dimensional methods has to be increased by a factor of at least ten. On the other hand, if the component of interest has at least one well-resolved ^{1}H NMR resonance then through the use of selective pulses it would be possible to carry out a 1-dimensional selective-excitation analogue of the 2-dimensional diffusion-edited TOCSY, COSY or NOESY experiments. Also a method has been proposed whereby the gradient strength and evolution time are incremented in concert (known as accordion spectroscopy) and this also reduces data acquisition time.[56]

Some of the measured diffusion coefficients are large in this study and it must be considered whether convection currents may be the cause (see Section 2.5). The temperature control unit of the spectrometer was maintained at nominally 37°C during the experiments and 128 dummy scans were used to obtain thermal equilibrium for the TOCSY experiment in order to obtain effective water resonance suppression. In addition the temperature internal to the sample was checked by using an NMR-thermometer method which has been published previously.[57] This is based on the temperature dependent chemical shift difference between water and the H1 proton of α-glucose and the actual internal temperature was determined to be 36.1°C. Based on the very small (<<1 Hz) differences seen throughout the experiments, any change in temperature during the measurements from beginning to end was less than 0.1°C. Thus whilst it is not possible to evaluate whether there are any time-independent temperature gradients along the NMR tube there appear to be no temperature changes during the experiments which could cause major temperature gradients.

The accuracy of the diffusion coefficients is of the same order as for conventional NMR T_1 and T_2 measurements, namely in the region of 5-10%. The highest level of accuracy will result if the analyte of interest has several ^{1}H NMR resonances which can be used to provide independent

determinations. This is the situation with glucose in blood plasma and the diffusion coefficient for α-glucose has an average value of 7.8×10^{-10} m^2s^{-1} and β-glucose has an average value of 7.6×10^{-10} m^2s^{-1}. Taking the two values as equal, since the α-β mutarotation rate is probably comparable to the diffusion time, leads to an average value for glucose of 7.7×10^{-10} m^2s^{-1} for seven measurements with a standard deviation of 0.8×10^{-10} m^2s^{-1}, i.e. close to 10%.

The derived molecular diffusion coefficients represent averages over the environment in which the analytes sample during the diffusion period of 300 ms. Thus, the observed diffusion coefficient provides a probe for investigating molecular interactions in complex mixtures such as biofluids. In particular, the rapid-exchange binding of endogenous small molecules to biofluid macromolecules can be studied and there is potential to study xenobiotic ligand-macromolecule interactions in biofluids including plasma.

3.3 Drug-protein binding

Many orally administered drugs, particularly those with ionizable groups, are bound extensively to human serum albumin (HSA) in blood plasma often with high affinity binding at one site and high capacity/low affinity binding at other sites.[58] In the case of many non-steroidal anti-inflammatory drugs the latter type of binding may be extensive with > 99% of the compound bound to HSA in blood plasma after oral administration and this binding can therefore affect drug distribution, therapeutic effect, toxicity and pharmacokinetics.[59] Many drugs bind tightly at a number of specific binding sites on albumin known as the "warfarin" and "benzodiazepine" sites because of the compounds first used to probe them.[60] This tight specific binding of drugs to proteins can be measured in a number of ways including x-ray crystallography, NMR nuclear Overhauser effect studies or the use of radio-labeled drug. However, the weaker binding interactions that usually involve many drug molecules bound to each protein molecule are more difficult to characterize than tight binding interactions. Traditionally weak protein binding has been studied using equilibrium dialysis,[61] ultrafiltration,[62] HPLC[63] or spectroscopic approaches monitoring a change in a spectroscopic parameter as a function of drug to protein proportions.[64] The separation methods rely on an assumption that the binding equilibrium is not perturbed by the measurement and that no drug is lost in the separation system. On the other hand, most spectroscopic methods rely on the assumption that all of the binding modes give rise to spectroscopic changes.

We have described the evaluation of the binding of a series of carboxylate compounds to HSA using as a probe of the interaction, the molecular diffusion coefficient of the drug.[20] Being a whole molecule property, this does not suffer from the disadvantage of other spectroscopic parameters as being potentially insensitive to certain binding modes. To investigate the usefulness of this approach to study protein-ligand binding, we used a model system with a fluorine-containing ligand, 4-trifluoromethylbenzoic acid (TFBA) **(1)**, since fluorinated compounds are widely used as drugs and novel therapeutic agents and ^{19}F NMR spectroscopy is also employed extensively in drug metabolism studies. The study was extended by measurement of two non-steroidal anti-inflammatory drugs, R,S-ibuprofen **(2)** and R,S-flurbiprofen **(3)**, the structures of which are given on Figure 5, and which are known to be extensively bound to HSA in blood plasma.[58]

The NMR parameters of the ligand, such as chemical shifts and relaxation times (T_1 and T_2), generally change on binding to a protein, and there is usually difficulty in using NMR spectroscopy to study protein-ligand binding

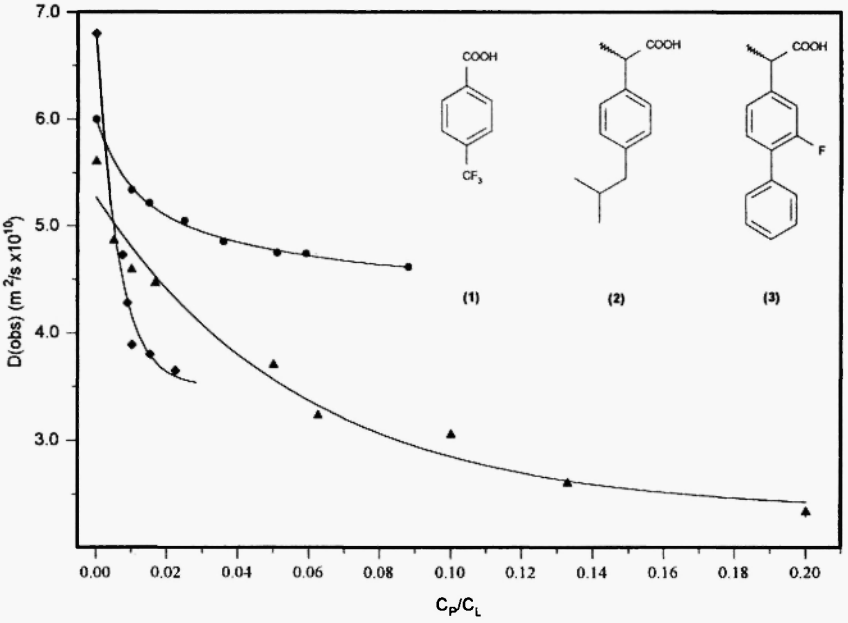

Fig. 5: The dependence of the observed ligand diffusion coefficient, D_{obs}, as a function of the HSA to ligand concentration ratio (C_P/C_L). ▲ - TFBA **(1)**, ● - ibuprofen **(2)**, and ◆ - flurbiprofen **(3)** .

directly. This is because of the need to extrapolate the observed NMR parameters to obtain their values in the bound states. If there are several binding sites, there will be, in principle, different values for the NMR parameters at each binding site. Alternatively, these can be used as variable parameters in a curve fitting process, but this increases the degrees of freedom considerably such that errors on binding equilibrium constants become large. However, the diffusion coefficient is a molecular property which does not depend on the binding position, and the value of the diffusion coefficient of the bound ligand is equal to that of the fully saturated protein-ligand complex and this can be determined from resonances of the protein or ligand. There is a further benefit of using ^{19}F NMR spectroscopy to monitor the diffusion coefficient of fluorine-containing ligands since there are no background signals as would be the case for ^{1}H NMR measurements.

The rates of the protein-ligand exchange processes need to be taken into account when considering the interpretation of the effects of the gradients on the NMR signal intensities in the LED experiment.[65] However, an average diffusion coefficient results if the process is in fast exchange on the NMR diffusion time scale. Furthermore, if the relaxation times of the free and bound ligand are very different such that different fractions of free and bound ligand are visible by NMR spectroscopy, then the relative spin-spin relaxation times must be taken into account.[29,30]

For a binding equilibrium with an exchange rate that is fast on the NMR time scale, the observed NMR parameter is given by a weighted average of the values for the free and bound forms. Many ligands will also experience a 1:1 tight binding to HSA at the known high affinity binding sites and this binding in most cases will be in slow exchange on the NMR time scale. This will produce a very minor perturbation to any measurement of the HSA diffusion coefficient based on HSA resonances but will not contribute to those signals from the ligand which are indicative of binding in fast exchange on the NMR time scale.

In the simplest case, it can be assumed that all of the binding sites are independent, that the binding reaction at different sites is a first order reversible fast process and that all binding interactions have the same equilibrium dissociation constant K_d. The observed NMR parameter (the diffusion coefficient D_{obs}) is a weighted average of that for the free ligand, D_F, and that of the ligand-protein complex, D_B. Thus,

$$D_{obs} = (1 - x_B)D_F + x_B D_B \quad (5)$$

where x_B is the molar fraction of the ligand which is protein-bound. The fraction x_B can be expressed in terms of the number of binding sites, *n*, the dissociation constant, K_d and the total concentrations of ligand, C_L and protein, C_P such that

$$x_B = \alpha - [\alpha^2 - \beta]^{1/2} \quad (6)$$

where $\alpha = (C_L - K_d + nC_P)/2C_L$ and $\beta = nC_P/C_L$. Hence, in principle, the value of D_{obs} as a function of the ligand/protein concentration ratio can be used to derive the ligand-protein dissociation constant and stoichiometry of binding. The values of K_d and *n* and the limiting values of the observables, in this case D_B and D_F, are highly interdependent and often it is not possible to obtain realistic values of the parameters. In many cases only $n(D_B - D_F)/K_d$ can be determined.[66] Therefore, there is a desire for the measurement of empirical parameters which can describe the protein interaction in a model-free way and which can be used to derive predictive structure-binding relationships using other calculated physicochemical parameters. We used the logarithm of the concentration ratio of ligand to HSA which causes 50% of the drug to be bound and have termed this the saturation factor, $\log(SF_{50})$. Any suitable level of binding could be used and in different circumstances it might be preferable to use $\log(SF_{10})$ or $\log(SF_{90})$ for example.

The ^{1}H NMR diffusion coefficient measurements on the ligand-protein mixtures were carried out at 600 MHz using an instrument equipped with a field gradient accessory capable of delivering z-field gradients up to 630 $mT.m^{-1}$ or at 400 MHz using an instrument with a field gradient accessory capable of delivering z-field gradients up to 590 $mT.m^{-1}$. ^{19}F NMR diffusion coefficient measurements were carried out at 376.5 MHz. All measurements were made at 298K. Diffusion coefficient measurements were also carried out on solutions of (**2**) at various concentrations and temperatures in phosphate buffer at pH7.4 using ^{1}H NMR spectroscopy at 500 MHz in order to investigate possible aggregation in free solution. The field gradient values were calibrated by collecting a one-dimensional NMR image of a tube of water of known length. The pulse sequence used bipolar sine-shaped gradients and a fifth gradient was included to remove the phase distortion caused by spin-spin couplings. The WATERGATE[27] sequence was used for water resonance suppression. This is similar to the approach of Altieri *et al*[67] who employed a different water suppression sequence. The intensities of the

peaks were used for diffusion coefficient calculation using the standard two-parameter exponential fitting routine used for relaxation time determination. The diffusion coefficients were measured for the three compounds both in free solution and in solutions with a range of ligand to HSA concentration ratios.

The diffusion coefficients for the three compounds **(1)** - **(3)** are shown in Table 2.[20] All compounds are carboxylic acids and therefore may undergo dimerization or aggregation with the proportions of dimers depending on the solution concentration. We measured the diffusion coefficient of **(2)** in phosphate buffer at pH7.4 at two concentrations and at various temperatures to check for this. The temperature dependence of the diffusion coefficients of both **(2)** and dimethylformamide, added as a non-interacting standard, were the same and probably reflect viscosity changes in the solutions. Within the experimental error, the value of the diffusion coefficient of **(2)** was identical for the two concentrations of **(2)** at all temperatures. Thus, at least for this compound, there was no evidence for different proportions of monomers and dimers over the temperature range studied,

The apparent diffusion coefficients of the three compounds were also measured in the presence of 1 mM HSA, at various excess concentrations of the ligands. The HSA concentration was maintained constant and the ligand concentration varied so as to minimize viscosity changes in the solutions. The variation of the observed diffusion coefficient of each compound as a function of the HSA to ligand concentration ratio is shown in Figure 5. The apparent diffusion coefficients of the ligands are reduced as the amount of

Table 2

Diffusion coefficients and relative HSA binding of carboxylate compounds (1) - (3)

	D(free) $x10^{10}$ $m^2.s^{-1}$	D(bound) $x10^{10}$ $m^2.s^{-1}$	SF_{50}	$log(SF_{50})$
TFBA **(1)**	5.0	1.8	16	1.20
R,S-ibuprofen **(2)**	6.0	4.6	29	1.46
R,S-flurbiprofen **(3)**	6.9	3.6	144	2.16

SF_{50} is the ratio of the concentration of ligand to HSA solution which is required to give 50% of the drug bound.

bound ligand increases, until the protein is fully saturated with ligand. At this point the curve asymptotes to the diffusion coefficient of the protein-ligand complex. The values obtained for the fully-ligand-bound protein for each ligand are also given in Table 2.

The diffusion coefficient of HSA has also been measured in free solution and in the presence of the ligands. From the graphs or by fitting to a simple polynomial it is possible to extract the diffusion coefficient of HSA fully saturated with ligand (i.e. based on the derived diffusion coefficients of the ligand) and these are also listed in Table 2. It appears that the diffusion coefficient for **(2)** when fully saturating HSA is higher than that for **(1)** or **(3)**. This can be interpreted as a smaller number of molecules of ligand bound, given that the molecular weights of the compounds are similar. The shape of the diffusion coefficient graphs in Figure 5 for **(1)** and **(3)** are quite different and although they appear to asymptote to similar values when the HSA is fully saturated, the individual dissociation constants and binding stoichiometries must be rather different.

It is possible in principle to fit those data shown in Figure 5 to derive a value for K_d and n the dissociation constant and stoichiometry of the ligand binding assuming n equivalent sites of binding and this was done for **(1)**. The variation of the observed diffusion coefficient as a function of the ligand-protein ratio was fitted to yield values for K_d and n. The best fit value was for $K_d = 2.2 \times 10^{-3}$ mol with $n = 9$, and this yielded a diffusion coefficient for the bound ligand of 1.4×10^{-10} $m^2.s^{-1}$, identical to that measured using the HSA resonances for the **(1)**-HSA complex and close to the value of 1.8×10^{-10} $m^2.s^{-1}$ extrapolated from Figure 5 and given in Table 2. Accepting a value of $n = 9 \pm 1$, leads to a value for $K_d = 2.2 \times 0.3 \pm 10^{-3}$ mol.

Figure 6(a) shows the variation of the ^{19}F chemical shift and Figure 6(b) shows the variation in spin-lattice relaxation rate for **(1)** as a function of HSA concentration. Derivation of the binding constant from the variation of ^{19}F chemical shifts or spin-lattice relaxation times gave unrealistic results because of the uncertainty in the values of the parameters for the fully bound ligand **(1)**. However, when the binding constant and number of sites were taken from the diffusion data, and then used to fit the ^{19}F chemical shift and spin-lattice relaxation time variation, the values for the chemical shift difference between the bound and the free form was calculated to be 116.13 Hz and the bound relaxation time is 0.76 ± 0.01 s^{-1}. Both of these values are realistic as seen from the graphs of spin-lattice relaxation rate and chemical shift shown in Figure 6(a) and Figure 6(b) respectively. These show the variation in spin-lattice

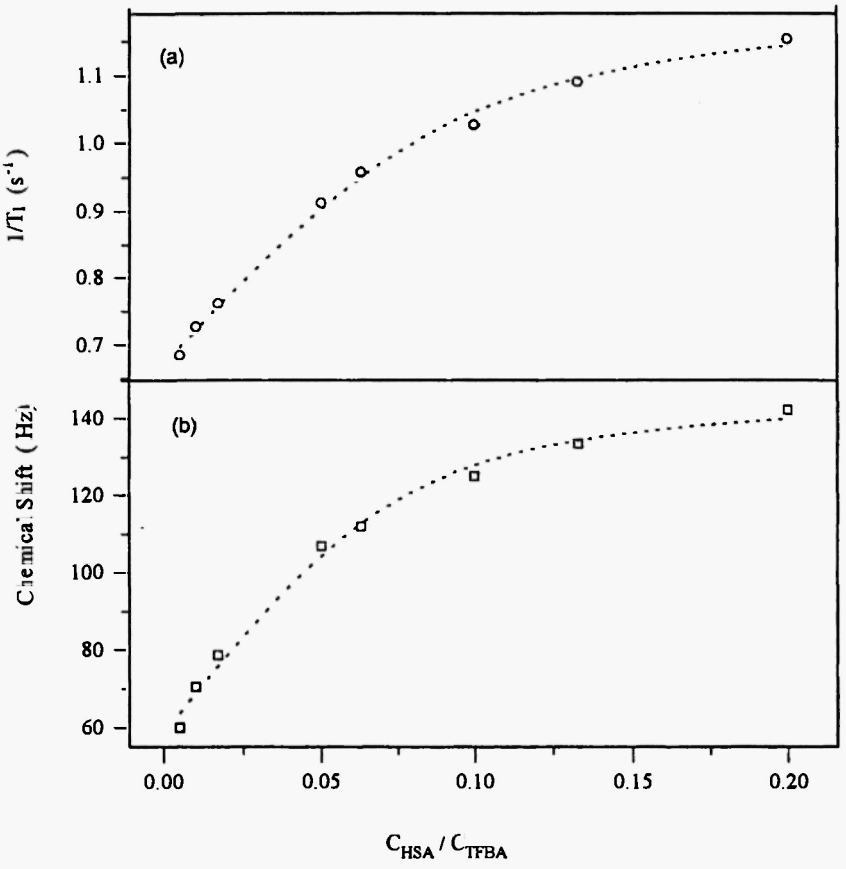

Fig. 6: Measurement of the binding of TFBA (**1**) to HSA using ^{19}F NMR chemical shift and ^{19}F NMR spin lattice relaxation rate, (a) the ^{19}F spin lattice relaxation rate of TFBA (**1**) as a function of the HSA/TFBA concentration ratio where the fitted line is used to derive the ^{19}F spin lattice relaxation rate of the bound form using the equilibrium dissociation constant, determined from the ^{19}F NMR diffusion coefficient measurement, of 2.2×10^{-3} mol. at 9 binding sites with the diffusion coefficient of the free ligand being 4.94×10^{-10} $m^2 \cdot s^{-1}$ and the diffusion coefficient of the bound ligand being 1.37×10^{-10} $m^2 \cdot s^{-1}$ and this gives T_1 of the free ligand as 1.51±0.02 s and T_1 of the bound ligand as 0.76±0.01 s, and (b) the ^{19}F chemical shift of TFBA (**1**) as a function of the HSA/TFBA concentration ratio where the fitted line is used to derive the chemical shift of the bound form using the binding equilibrium constant determined above and this gives a binding chemical shift of 116±13 Hz.

relaxation rates, T_1^{-1} (O) and chemical shift changes (□) as a function of the **(1)**:HSA ratio and the fitted results (dotted lines) were as calculated using the model above.

This demonstrates the difficulty of determining K_d and *n* from a single graph of diffusion coefficient (or, for that matter, chemical shift or relaxation rate) *versus* ligand concentration. This highlights the need for a model-free parameter. Having determined the free ligand diffusion coefficient and that for the ligand when the HSA is fully saturated, it is possible by interpolation to derive the fraction of ligand bound at any given ligand/protein concentration ratio. From this, it is then possible to derive a value for the concentration ratio at which 50% (or any other percentage desired) of the ligand is bound. Having defined the saturation factor of a protein as $\log(SF_{50})$, these values for compounds **(1)** - **(3)** are also given in Table 2.

The analysis assumes that the ligand is in fast exchange between free solution and the HSA on the chemical shift NMR time scale, the relaxation time scale and also the diffusion time scale. The fast exchange regime on the chemical shift time scale was confirmed by measurement of unchanged ligand NMR resonance integrals as a function of HSA concentration and the fast exchange on the diffusion time scale was ensured by using a diffusion time of 500 ms.

Several difficulties may be encountered when using ^{1}H NMR spectroscopy to measurement diffusion coefficients of small molecules in aqueous protein solutions. These include the necessity for a water resonance suppression scheme, the problem of chemical shift overlap of protein and ligand resonances and the broadening of the ^{1}H NMR resonances of the ligand caused by rapid relaxation. In this study, we also compared the ^{19}F NMR-based diffusion coefficient of **(1)** in the presence of HSA with the values obtained using ^{1}H NMR spectroscopy using a solvent resonance saturation scheme. At high ligand-protein concentration ratios, the diffusion coefficients measured by ^{1}H and ^{19}F NMR spectroscopy were the same within the experimental error. At lower **(1)**:HSA ratios, (<20:1), the ^{1}H signals of **(1)** become broadened because of the shorter average relaxation time and under these circumstances, the use of a multiple exponential fitting routine must be considered. At these lower ligand-HSA concentration ratios, the diffusion coefficient of the ligand determined using a single exponential decay is reduced by about 10%, as compared to the value determined using ^{19}F NMR spectroscopy. It should be noted that the diffusion coefficients measured using ^{1}H NMR spectroscopy in circumstances where the ligand and protein

resonances overlap are, as expected, lower than when measured using ^{19}F NMR spectroscopy because of the contribution to the peak intensity from the protein which has a lower value diffusion coefficient and consequently, leads to an underestimation of the dissociation constant.

The extrapolated value of the diffusion coefficient for the fully-bound ligand can yield information on the number of molecules bound to HSA. Thus, ignoring molecular weight differences between the ligands, from an examination of Figure 5, it appears that **(1)** and **(3)** have similar bound diffusion coefficients and hence similar numbers of molecules bound. On the other hand, **(2)** has a limiting diffusion coefficient that is considerably higher and indicates fewer molecules bound. From Table 2 it can be seen that **(1)** is extensively bound to HSA, requiring only a 16 fold excess of ligand to protein to achieve 50% saturation of the protein. The clinically used drugs **(2)** and **(3)** are less bound to HSA requiring 29 and 144 times respectively excess concentration of drug over HSA to achieve 50% saturation of the protein.

There is an additional complication that arises in the study of the racemic mixtures of **(2)** and **(3)**. The NMR spectra and diffusion coefficients of the enantiomers in free solution are identical but on binding to a chiral protein, if the binding of the two enantiomers is different, then the ligand enantiomers will have different average diffusion coefficients and in principle different average chemical shifts. We did not observe any differences in chemical shifts. In principle, in order to calculate the diffusion coefficients of the racemic mixture of ligands in the presence of HSA, it would be necessary to use a double exponential fit to the NMR intensity data. However, the data which we obtained could be fitted satisfactorily using only a single average diffusion coefficient and hence it was not possible to detect differential low affinity binding of the R and S enantiomers of **(2)** and **(3)**. Very recently, we have measured the binding of R- and S-ibuprofen separately to HSA using diffusion coefficient measurement and found no difference in the weak binding between the two enantiomers.[68]

In summary, the measurement of molecular diffusion coefficients offers a number of advantages over other NMR methods of measuring ligand-protein binding constants. The method described above is only applicable in situations where the ligand is in fast exchange with the receptor and a weighted-average diffusion coefficient is observed. The primary advantage of the method lies in the fact that it is not necessary to postulate values for bound ligand NMR chemical shifts, line widths or relaxation times for a single binding site or for multiple sites.

3.4 Impurity Characterization in Pharmaceuticals

The manufacture and quality control of a drug product is controlled by a variety of national regulatory authorities. There is a strong emphasis on the purity of final drug substances and registration authorities require full characterization and identification of any impurities at the level of 0.1% of the UV peak area using HPLC.[69] Currently, in order to characterize such impurities, it has proved necessary to isolate individual components by preparative HPLC and use NMR spectroscopy and mass spectrometry for structural identification. This work is often time consuming and expensive but even so may not always be conclusive. We recently showed that directly-coupled HPLC-NMR spectroscopy can provide a more efficient method for this type of study and this has recently been applied to characterize a number of impurities in a partially purified batch of fluticasone propionate **(4)** which has the chemical structure shown in Figure 7.[70] There is, however, a considerable need to develop and validate new methods for determining product purity. With this aim, we applied ^{19}F NMR spectroscopy to the measurement of molecular diffusion coefficients of the mixture components in a partially purified batch of **(4)** to provide a distinction between monomeric and dimeric substances without the need for HPLC separation.[71]

High resolution ^{19}F NMR spectroscopy is potentially an excellent method for product profiling for substances containing fluorine since the C-F bond is strong and degradative defluorination is relatively rare. In addition, it is likely that any related impurities or degradation products of the drug will also contain fluorine. The ^{19}F nucleus is 100% abundant, with spin = ½, and a large magnetic moment[72] which results in ^{19}F NMR spectroscopy being a very sensitive method of detecting minor fluorine-containing compounds in a bulk production sample of a pharmaceutical material. It is possible to use ^{19}F NMR spectroscopy to determine the number of different fluorine-containing components present in a mixture by counting the number of different fluorine peaks in a spectrum around a specific chemical shift region. Provided that the ^{19}F NMR spectrum is acquired under conditions of full T_1 relaxation, it is possible to quantify the relative amounts of the different components in the mixture by measuring integrals or peak heights of the minor fluorine peaks in the spectrum.

A mixture of authentic standard compounds was prepared comprising 2.5 mg of **(4)** and **(5)** and 5 mg of **(6)** and **(7)** in 0.7 mL dmso-d_6. The test sample

of fluticasone propionate was obtained from a partially purified batch of the drug substance prior to formulation and a solution of 20 mg dissolved in 0.7 mL dmso-d_6 was prepared. This contained a number of components related to **(4)** at varying levels, some of which were dimers and others monomers. Some of the key structures are shown in Figure 7.

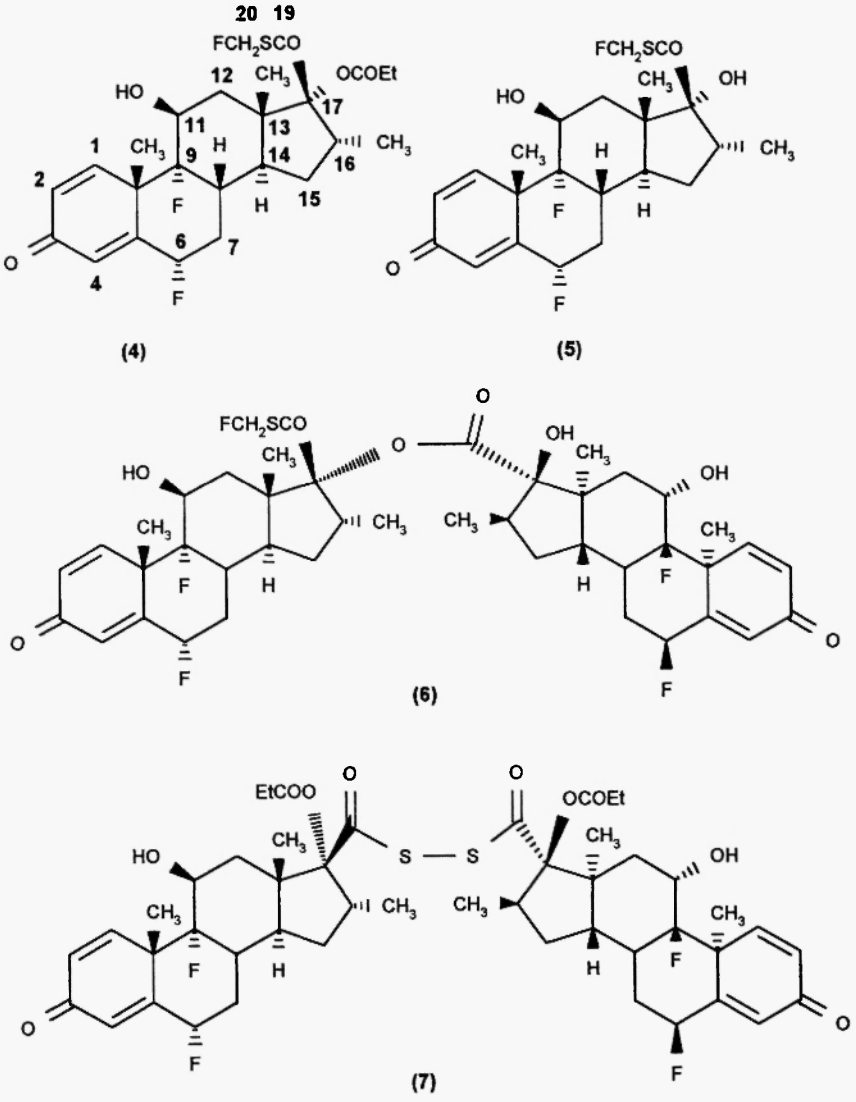

Fig. 7: Structures of fluticasone propionate **(4)** and related model monomer and dimer compounds. The atom numbering is as shown.

The ^{19}F NMR spectroscopic data were acquired at 376.50 MHz and at a temperature of 303K using a spectrometer equipped with a 5mm, 4-nucleus, $^{1}H/^{19}F/^{13}C/^{31}P$ probe containing field-gradient coils and a gradient unit capable of delivering magnetic field gradient pulses along the magnetic field direction with strengths up to 590 $mT.m^{-1}$. ^{19}F NMR spectra were obtained with ^{1}H decoupling ($^{19}F-\{^{1}H\}$ spectra) using the WALTZ method.[73] Measurement of molecular diffusion coefficients was achieved using the bipolar-gradient LED method for ^{19}F NMR. The peak intensities were measured for 32 values of the field gradient and the 24 most intense peaks in the ^{19}F NMR spectrum were used for the diffusion coefficient calculation. A diffusion coefficient was calculated for each ^{19}F NMR resonance.

The $^{19}F-\{^{1}H\}$ NMR spectrum of the batch of fluticasone propionate in dmso-d_6 is given in Figure 8 showing an expansion of the region around δ_F -164.[71] The peaks have been numbered and the chemical shifts are given in Table 3. The peaks in this region arise from F-9 of **(4)** and related compounds. In addition, there are a number of peaks around δ_F -186 and these

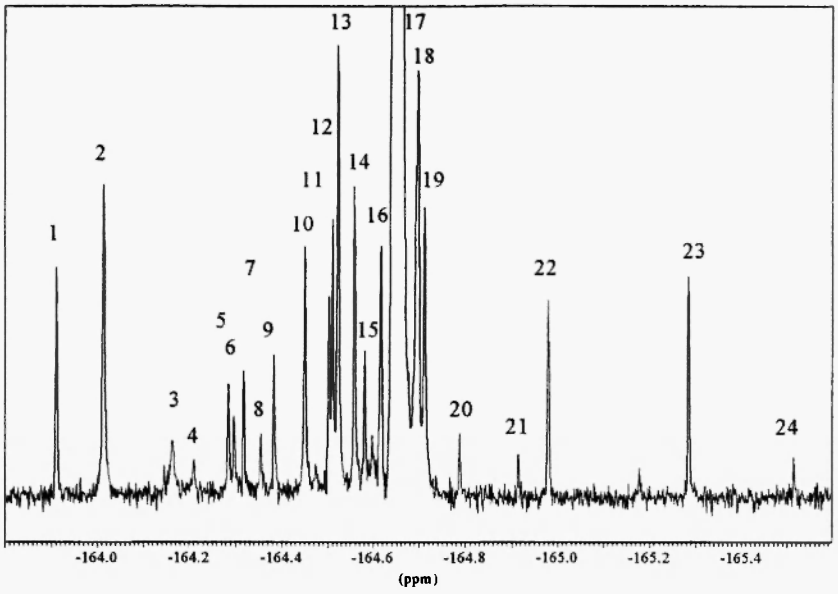

Fig. 8: ^{19}F NMR spectrum of a batch of bulk fluticasone propionate **(4)** showing expansions of the region δ_F -163.8 to δ_F -165.6 where the peaks arise from F-9 in **(4)** and related molecules. Assignments are given in Table 3.

Table 3

^{19}F NMR chemical shifts, mole% and diffusion coefficients of components of the partially purified batch of fluticasone propionate (4).

Peak	Chemical shift (δ_F)	Mole%	Diffusion Coefficient ($x10^{10}$ $m^2.s^{-1}$)	Identity
1	-163.91	0.28	2.63	
2	-164.01	0.47	1.93	dimer
3	-164.16	0.09	a	
4	-164.21	<0.09	a	**(7)** dimer
5	-164.29	0.19	a	**(8)** monomer
6	-164.30	0.09	a	**(5)** monomer
7	-164.32	0.19	a	
8	-164.36	0.09	a	**(9)** monomer
9	-164.38	0.219	2.44	**(10)** monomer
10	-164.45	0.38	2.00	
11	-164.50	0.28	2.69	
12	-164.51[b]	0.38	2.54	**(4)** monomer
13	-164.52	0.66	2.00	**(7)** dimer
14	-164.56	0.47	2.35	
15	-164.58	0.19	2.40	**(11)** monomer
16	-164.62	0.38	2.31	
17	-164.65	94.07	2.54	**(4)** monomer
18	-164.70	0.56	2.48	
19	-164.71	0.38	2.44	
20	-164.78	0.09	a	
21	-164.92	<0.09	a	
22	-164.98	0.28	2.66	
23	-165.28[b]	0.28	2.96	**(4)** monomer
24	-165.51	<0.09	a	**(7)** dimer

a - Signal-noise ratio inadequate for diffusion measurement

b - ^{13}C satellites of **(4)**

(8) - As **(4)** but with OH and COOH substituted at C-17; **(9)** as **(4)** but with oxathiazole substituted at C-17; **(10)** as **(4)** but with COSH and COOEt substituted at C-17; **(11)** as **(4)** but with H and COOH substituted at C-17

arise from the corresponding F-6 nuclei (see Figure 7). Also, **(4)** itself has an additional resonance at δ_F -191.98 ppm arising from the CH_2F group. The ^{13}C satellite peaks of **(4)** were identified at δ_F -164.51 and δ_F -165.28. The mole% for each of these components based on ^{19}F NMR was calculated and these values are also given in Table 3. There was good agreement for **(4)** itself between values obtained by ^{19}F NMR spectroscopy and HPLC with UV detection. Some impurities have been identified using directly-coupled HPLC-NMR and HPLC-MS[70] and Table 3 indicates the structure of these compounds and whether the materials were monomeric or dimeric.

Diffusion coefficient measurement has been used to investigate whether it was possible to discriminate by NMR which impurities were dimeric.[71] The diffusion coefficients of the standard compounds are given in Table 4 for each ^{19}F resonance. There was good consistency in values for different resonances in the same molecule and for monomers and dimers. Table 4 shows that the monomeric substances **(4)** and **(7)** had diffusion coefficients of ca. 2.1×10^{-10} $m^2.s^{-1}$ whilst the dimers had values of ca. 1.6×10^{-10} $m^2.s^{-1}$.

Diffusion coefficients were then measured for each ^{19}F NMR resonance arising from the bulk batch of **(4)**. The determined diffusion coefficients are also given in Table 3. The absolute values of the diffusion coefficients for each molecule differ somewhat from the values determined in the simple

Table 4

NMR-determined diffusion coefficients for (4) - (7)

Identity	Chemical Shift (δ_F)	Diffusion Coefficients ($\times 10^{10}$ $m^2.s^{-1}$)
(6)	-164.22	1.61
(6)	-164.31	2.17
(7)	-164.52	1.55
(4)	-164.64	2.16
(7)	-165.53	1.61
(6)	-186.51	1.65
(5)	-186.55	2.16
(6), (7)	-186.71	1.58
(4)	-186.74	2.07

Note that **(4)** and **(5)** are monomeric and **(6)** and **(7)** are dimeric.

mixture of four compounds and this is probably due to differences in sample viscosity. Nevertheless, there is a clear distinction between the known monomer and dimer species. There is evidence from the diffusion coefficient data for the presence of 3 different dimers amongst the major impurity peaks in the ^{19}F NMR spectrum around δ_F -164. These are peaks 2, 10 and 13 in Table 1 of which peak 2 is known to be dimeric and peak 13 is also the dimer molecule (7).

Measurement of diffusion coefficients using the well-resolved resonances in a ^{19}F NMR spectrum of a mixture can therefore be a useful initial technique for distinguishing the components according to their relative mobility and hence molecular size. In the present case, where one molecule dominates, the most accurate values will be determined for the main component fluticasone propionate itself as it represents about 94% of the total material. However, because of the lower signal-noise ratio of the NMR peaks from the impurity components, it is expected that the derived diffusion coefficients of the minor impurities will be less precise.

3.5. Solvent accessibility of protein and peptide NH groups

One of the standard experiments conducted during NMR studies of protein structure is to measure the temperature dependence of NH proton chemical shifts.[74] Exchangeable protons with negligible temperature coefficients are regarded as having low accessibility to the solvent water. However, this requires the measurement of spectra at elevated temperatures with the consequent possibility of degradation or denaturation of the protein or peptide. The relative exchange rates of protons on NH groups can also be determined using exchange experiments with D_2O at a single temperature but this can produce deuteration of other exchangeable protons such as CH protons in histidinyl residues. Variations in pH of the sample also influence the exchange rate of solvent-accessible labile protons, but in addition extremes of pH may result in changes to peptide conformation or in denaturation of proteins. Consequently, an experiment which gives access to information on NH exchange in a non-invasive way is desirable and there are a number of approaches in the literature, including transfer-of-saturation experiments and 2-dimensional NMR methods such as NOESY and EXSY[74] and selective water resonance inversion.[75]

Another possibility is to measure the apparent diffusion coefficients of the various NH protons as these will reflect the relative lifetimes of the protons

on the peptide and on the solvent water. This approach has been tested using the exchange of protons between *N*-acetylaspartate and water[76] and for proton exchange in a synthetic 16 base-pair DNA fragment.[77] Recently, a method based on a combination of a spin-echo diffusion sequence and a selective inversion ^{1}H-^{15}N HMQC experiment has been proposed and applied to water-amide exchange in acyl carrier protein.[78]

The problems of measuring diffusion coefficients in the presence of chemical exchange which can occur in the diffusion period in the LED sequence have also been addressed.[65] Consideration has to be given as to whether the spin system is in fast or slow exchange in terms of all NMR parameters including chemical shifts, relaxation times and now diffusion coefficients. The situation where a nucleus is in two environments but gives rise to only one chemical shift, i.e. fast exchange in chemical shift terms has been addressed specifically.[65] It has been shown that if diffusion is slow compared to the diffusion period, then the gradient squared dependence of the peak intensity is bi-exponential and two diffusion coefficients result but, if diffusion is fast, then a weighted average diffusion coefficient results as was seen for the HSA-ligand binding studies in Section 3.3. The situation where the chemical shifts of the exchanging species are in slow exchange has also been considered.[29] Here, if the diffusion period is long, then each of the sites will give separate chemical shifts and the apparent diffusion coefficients of the species at each site will be a weighted average of the diffusion coefficients of the species according to their relative populations. It has also been shown[30] that it is important to take into account the relative relaxation times of the nuclei at the exchanging sites if this would result in some of the spectral intensity becoming "NMR-invisible" as when binding to a macromolecule or a cell membrane.

The specific case of exchange between non-equivalent sites was first treated in a method named gradient-enhanced exchange spectroscopy (GEXSY) where the apparent diffusion behavior of exchangeable protons was explored using both 1-dimensional and 2-dimensional NMR experiments.[76] For intramolecular exchange, between water and an NH group of a peptide, which is in the fast exchange limit during the diffusion period but in slow exchange in chemical shift terms, the NMR cross-peak intensities show exponential behavior as a function of gradient strength squared. In the fast exchange limit, the observed D_{obs} is the average of that for the water (D_w) and peptide environments (D_p) weighted by the relative lifetimes of the proton on

water (f_w) and on the peptide (f_p). The probability that no exchange has taken place out of the peptide site is exp ($-1/\tau_p$) if τ_p is the lifetime of the proton in site p. Here we define $f_p = \tau_p/(\tau_p + \tau_w)$ as the fractional time that a proton stays in the p site during the diffusion time.

However, if the fast exchange limit is not obeyed, distinction needs to be made between spins which exchange during the diffusion period and those which do not. Thus outside the fast and slow exchange limits and when $\tau_p << \tau_w$, it has been shown[76] that the gradient dependence of a resonance intensity is given by Equation (7)

$$I_i = I_{0i} \{\exp(-K^2 D_w \Delta) - P \exp(-K^2 D_p \Delta)\}/\{[1 - K^2 (D_w - D_p) f_p \Delta][1 - P]\} \quad (7)$$

Here K is $\gamma_i G\delta$, where γ_i is the spin magnetogyric ratio, G and δ are the strength and duration of the field gradient, and Δ is the diffusion period. We have tested this general approach but in a non-selective 1-dimensional NMR mode using the peptide antibiotic viomycin, which has been used in the treatment of tuberculosis. The first study of NH exchange in viomycin in aqueous solution derived full assignments and made studies of the NH solvent accessibility as a function of pH by the one-dimensional saturation transfer method.[79] A later study using the two-dimensional NOE method also derived NH exchange rates.[80] The molecular structure and numbering scheme for viomycin is shown in Figure 9 and this peptide has now been studied as a

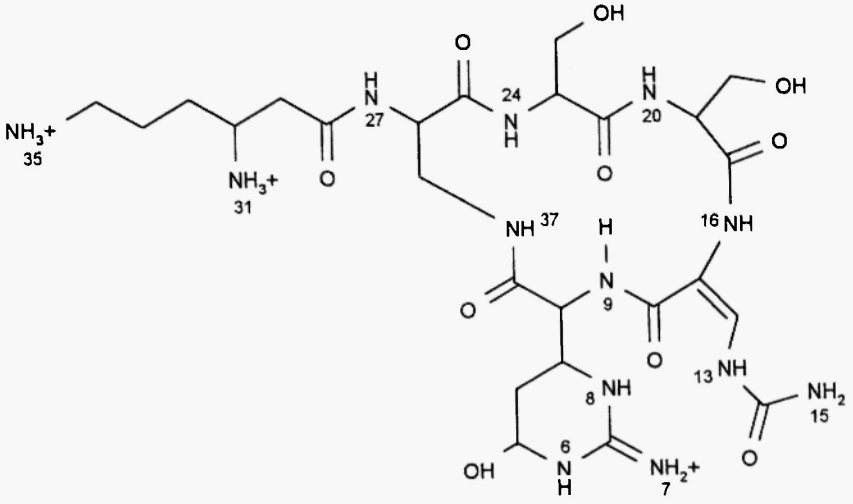

Fig. 9: The structure and numbering system for viomycin.

model system to investigate the feasibility of NMR diffusion measurements of apparent differential diffusion of NH protons as a measure of their accessibility to the solvent water. In the absence of ^{15}N labeled viomycin, a non-selective method based on ^{1}H NMR spectroscopy with non-excitation of the water resonance has been used. The initial study was used to demonstrate the feasibility of the use of relative diffusion coefficient measurements for investigating NH exchange in peptides and proteins.

All NMR spectra were measured on a spectrometer operating at 600 MHz for ^{1}H observation and using a gradient unit capable of providing gradients up to 2000 $mT.m^{-1}$ along the magnetic field direction. The data were acquired with a version of the LED delay pulse sequence with the inclusion of the WATERGATE solvent peak suppression scheme[27] to eliminate the resonance of the water without causing any transfer of saturation. A series of spectra were measured for values of the gradient strength in the range 20 $mT.m^{-1}$ – 700 $mT.m^{-1}$ in random order in steps of 20 $mT.m^{-1}$ using bipolar sine-shaped gradients of base length 2 ms with a diffusion period of 300 ms.

The expression P in Equation [7] is equal to $\exp(-\Delta/f_p)$ where f_p is the fractional lifetime of the exchangeable hydrogen on the peptide during the diffusion period which is equal to $(\Delta - 5\delta/16 - \tau/2)$ for sine-shaped gradients where τ is the time between the two bipolar gradient components. Thus Equation [7] can be reformulated as

$$I_i = A_{0i}\{\exp(-K^2D_w\Delta) - P\exp(-K^2D_p\Delta)\} \quad (8)$$

where $A_{0i} = I_{0i}/\{[1 - K2(D_w - D_p)f_p\Delta][1 - P]\}$.

The pulse sequence used here was a non-selective 1-dimensional experiment and, unlike in the case of the 2-dimensional GEXSY approach,[76] it is not possible to separate the exchanged part of an NH peak from the non-exchanged part during the diffusion period. Thus the observed intensity of an NH resonance in the diffusion measurement NMR experiment used here will comprise two components, an exchanged (E) part which transferred from water during the diffusion period and a non-exchanged (N) part, corresponding respectively to the cross-peak and diagonal peak of the GEXSY experiment. In the fast exchange limit, the E and N components are affected by the magnetic field gradients according to Equations (9) and (10) respectively.

$$I(E)_i = I(E)_{0i} \exp\{[-K^2(D_w f_w + D_p f_p)\,\Delta]\} \quad (9)$$

$$I(N)_i = I(N)_{0i} \exp\{-K^2 D_p \Delta\} \quad (10)$$

Thus, since the components are not separated in the 1-dimensional NMR experiment, the total intensity attenuation is bi-exponential.

$$I_i = I(E)_{0i} \exp\{[-K^2(D_w f_w + D_p f_p)\,\Delta]\} + I(N)_{0i} \exp\{-K^2 D_p \Delta\} \quad (11)$$

The observed NH resonance intensities were fitted to equation [11] to yield the relative lifetimes. The diffusion coefficient of viomycin was obtained by averaging values based on twelve CH NMR resonances and that from water was taken from the water resonance intensity. The results were normalized to the known diffusion coefficient of water[82] at 2.30×10^{-9} $m^2.s^{-1}$.

The 600 MHz ^1H NMR spectra of viomycin in H_2O/D_2O using the LED pulse sequence are shown in Figure 10. The spectrum given in Figure 10(a) shows the region that includes all of the NH resonances and the olefinic CH resonance and was obtained with a very low gradient value of 20 $mT.m^{-1}$; this is essentially identical to a conventional spectrum. The CH resonance which appears at δ7.9 is complicated by the fact that it comprises a doublet from molecules with a CH.NH moiety and an overlapping singlet from viomycin molecules containing a CH.ND moiety in slow exchange with each other. The assignment of the NH resonances has been achieved previously and is as given in Table 1 according to the scheme shown in Figure 9.[79]

Figures 10(b) - (e) show the same region of the spectrum but acquired with increasing values of the strength of the magnetic field gradient. All of the NMR resonances are diminished in intensity as the gradient strength is increased. However, the effects are not constant for all of the peaks, and those in fastest exchange with the water are attenuated first. The NH resonances from the NH_3^+(31,35) groups do not appear in the spectrum using only a 20 $mT.m^{-1}$ gradient and therefore these are the groups in fastest exchange with the water. From a qualitative inspection of the spectra, the next fastest to exchange is NH(6) from the six-membered ring and this has been virtually eliminated from the spectrum using a gradient level of 200 $mT.m^{-1}$. There are four NH groups which are next most susceptible to loss of intensity and these are NH(16), NH(27), NH(8) and NH_2^+(7). The next fastest proton in order of exchange rate is NH(13) and somewhat slower is NH(20). The signal from NH(24) attenuates at higher gradient strength and then there is a final group

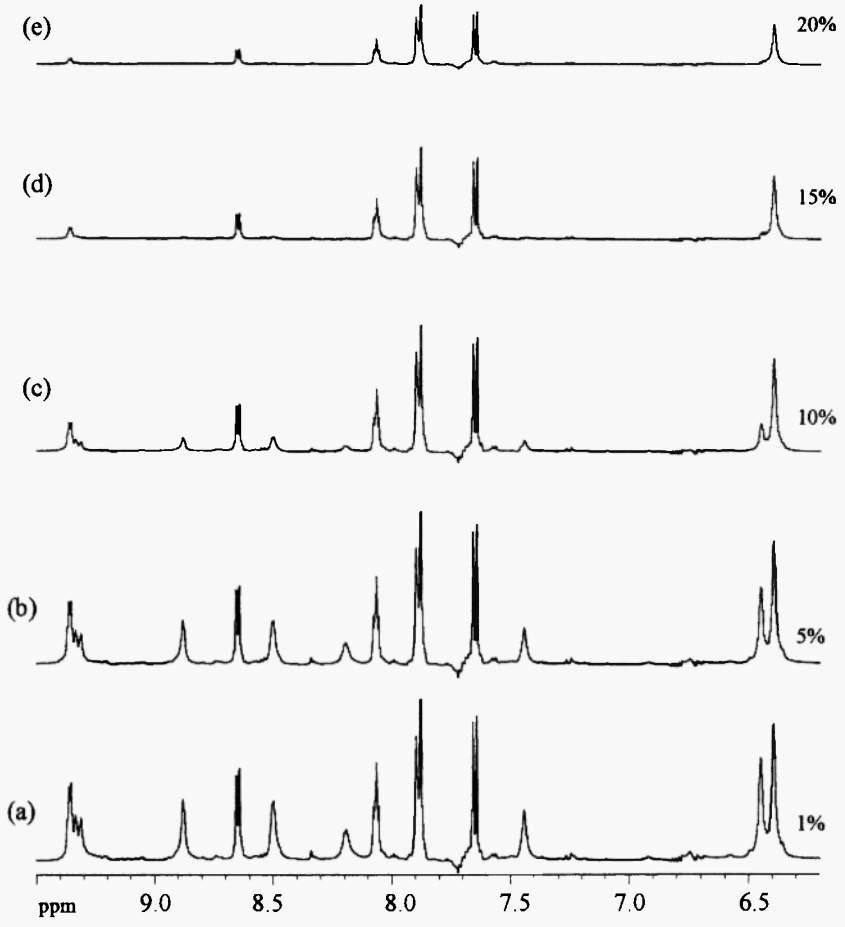

Fig. 10: 600 MHz ^{1}H NMR spectra of the NH region (δ6.2 - δ9.5) of the spectrum of viomycin in H_2O/D_2O, 90/10 *v/v* at various gradient strengths using the LED pulse sequence with WATERGATE non-excitation of the water resonance. The assignments are given in Table 5, (a) 20 $mT.m^{-1}$ (b) 100 $mT.m^{-1}$ (c) 200 $mT.m^{-1}$ (d) 300 $mT.m^{-1}$and (e) 400 $mT.m^{-1}$.

where the attenuation caused by the gradient is considerably less. These protons therefore have less solvent accessibility and of this group, NH(37) and NH_2(15) lose intensity somewhat faster than the others. Three proton signals decrease in intensity least as a function of the gradient and these are the two signals from the =CH group and that from the NH(9) group. The

attenuation of the =CH signals is representative of the overall diffusion of the whole molecule as this proton is not in exchange with the solvent water. The NH(9) proton has a gradient-related attenuation which is very similar to that of the overall molecule and thus this NH group has very little solvent accessibility on the time scale of the diffusion period consistent with it being part of an intramolecular hydrogen bond as found.[79,80,83] In addition, the signals from NH(37) and NH_2(15) also show slow diffusion characteristics and therefore these groups must also have considerably restricted access to the solvent.

The qualitative results described above have been refined by calculation of the proton lifetimes on the peptide based on the various viomycin CH and NH resonances. The diffusion coefficient of viomycin was obtained as the mean value of twelve resonances in the aliphatic region of the spectrum with the value 2.73×10^{-10} $m^2.s^{-1}$. Since there is a large concentration excess of water over peptide, the diffusion coefficient of water can be considered as independent of the exchange process and this was obtained from a separate experiment without solvent suppression and provided a value of 2.30×10^{-9} $m^2.s^{-1}$. The NH proton peak intensities were fitted to Equation (11) as described above to yield values for f_p the lifetime of the proton on the peptide, using values of D_p and D_w above. The derived values are given in Table 5.

Thus, based on diffusion measurement, the relative NH lifetimes are NH(9) >> NH(15) NH(37) ≈ NH(24) > NH(20) > NH_2^+(7) > NH(27) ≈ NH(13) ≈ NH(16) > NH(8) ≈ NH(6) and finally the NH_3^+ groups. This order is in good agreement with previous work based on pH variation and saturation transfer experiments[79] and is also consistent with a study based on two-dimensional NOESY experiments when quantitative values for exchange rate constants (in s^{-1}) were obtained for some protons *viz*, NH(8), 1.45 > NH(16), 1.21, NH(13), 1.18 > NH(27), 0.75 > NH_2(15), 0.52 > NH(20), 0.44 > NH_2^+ (7), 0.39 > NH(24), 0.13, but values for NH(16) and NH(37) could not be determined.[80]

The diffusion NMR method provides a rapid method for studying NH exchange rates without the need for D_2O addition or experiments at elevated temperatures. The method can easily be extended to a three-dimensional version with diffusion coefficient on the third axis, such as a ^1H-^{15}N HMQC or HSQC experiment.

Table 5
Chemical Shifts and Fractional NH Lifetimes of Hydrogens in Viomycin During the Diffusion Period

Assignment	Chemical shift (δ)	Lifetime on the peptide (ms)
NH(20)	9.36	102
NH(13)	9.31	60
NH(16)	8.88	57
NH(24)	8.66	120
NH(27)	8.50	66
NH(6)	8.19	0
NH(37)	8.07	129
CH	7.89	300
NH(9)	7.65	247
NH(8)	7.44	33
NH_2^+(7)	6.45	90
NH_2(15)	6.39	126
H_2O	4.67	-

4. REFERENCES

1. P. Stilbs, *Prog. NMR Spectrosc.*, **19**, 1 (1987).
2. E.O. Stejskal and J.E. Tanner, *J. Chem. Phys.*, **42**, 288 (1965).
3. E.L. Hahn, *Phys. Rev.*, **80**, 580 (1950).
4. J.E. Tanner, *J. Phys. Chem.*, **52**, 2523 (1970).
5. J.M. Fauth, A. Schweiger, L. Braunschweiler, J. Forrer, and R.R. Ernst, *J. Magn. Reson.*, 66, 74 (1986).
6. S.J. Gibbs and C.S. Johnson, Jr., *J. Magn. Reson.* **93**, 395 (1991).
7. D. Wu, A. Chen and C.S. Johnson, Jr., *J. Magn. Reson.*, **A115**, 260 (1995).
8. K.F. Morris, and C.S. Johnson, Jr., *J. Am. Chem. Soc.*, **115**, 4291 (1993).
9. D.P. Hinton and C.S. Johnson Jr., *J. Phys. Chem.*, 97, 9064 (1993).
10. M. Lin and M.J. Shapiro, J. Org. Chem., 61, 7617 (1996).

11. M. Lin, M.J. Shapiro and J.R. Wareing, *J. Am. Chem. Soc.*, **119**, 5249 (1997).
12. M. Lin, M.J. Shapiro, and J.R. Wareing, *J. Org. Chem.* **62**, 8930 (1997).
13. A. Gafni and Y. Cohen, *J. Org. Chem.*, **62**, 120 (1997).
14. D.P. Hinton and C.S. Johnson Jr., *Chem. and Phys. Lipids*, 69, 175 (1994).
15. A. Chen, D. Wu and C.S. Johnson Jr., *J. Am. Chem. Soc.*, **117**, 7965 (1995).
16. H. Barjat, G.A. Morris, S. Smart, A.G. Swanson and S.C.R. Williams, *J. Magn.Reson.*, **108**, 170 (1995).
17. A.S. Altieri, D.P. Hinton and R.A. Byrd, *J. Am. Chem. Soc.*, 1995, **117**, 7566 (1995).
18. A.J. Dingley, J.P. Mackay, G.L. Shaw, B.D. Hambly and G.F. King, *J. Biomol. NMR*, **10**, 1 (1997).
19. N. Gonnella, M. Lin, M.J. Shapiro, J.R. Wareing and X. Zhang, *J. Magn. Reson.*, **131**, 336 (1998).
20. M. Liu, J.K. Nicholson and J.C. Lindon, *Anal. Comm.*, **34**, 225 (1997)
21. J.A. Jones, D.K. Wilkins, L.J. Smith and C.M. Dobson, *J. Biomol. NMR*, **10**, 199 (1997).
22. M. Lin and C.K. Larive, *Anal. Biochem.*, **229**, 214 (1995).
23. A. Chen, D. Wu and C.S. Johnson Jr., *J. Phys. Chem.*, 99, 828 (1995).
24. S.S. Pochapsky, H. Mo and T.C. Pochapsky, *J. Chem. Soc. Chem. Comm.*, 2513 (1995).
25. M. Liu, J.K. Nicholson and J.C. Lindon, *Anal. Chem.*, **68**, 3370 (1996).
26. M. Liu, J.K. Nicholson, J.A. Parkinson and J.C. Lindon, *Anal. Chem.*, 69, 1504 (1997).
27. M. Piotto, V. Saudek and V. Sklenar, *J. Biomol. NMR*, **2**, 661 (1992).
28. D. Wu, A. Chen and C.S. Johnson, Jr., *J. Magn. Reson.*, **A123**, 215 (1996).
29. A.J. Lennon, N.R. Scott, B.E. Chapman and P.W. Kuchel, *Biophys. J.*, 67, 2096 (1994).
30. A.J. Lennon, B.E. Chapman and P.W. Kuchel, *Bull. Magn. Reson.*, **17**, 224 (1996).
31. M. Liu, X.-A. Mao, C.-H. Ye, J.K. Nicholson and J.C. Lindon, *Mol. Phys.*, **93**, 913 (1998).
32. E.K. Gozansky and D.G. Gorenstein, *J. Magn. Reson.*, **B111**, 94 (1996).
33. D. Wu, A. Chen and C.S. Johnson, Jr., *J. Magn. Reson.*, **A121**, 88 (1996).

34. M.F. Lin and M.J. Shapiro, *Abstr. 37th ENC*, 1996, Asilomar, CA, USA.
35. H. Barjat, G.A. Morris and A.G. Swanson, *J. Magn. Rson.*,**131,** 131 (1998).
36. A. Jerschow and N. Muller, *J. Magn. Reson.*, A**123**, 222 (1996).
37. W.J. Goux, L.A. Verkruyse and S.J. Salter, *J. Magn. Reson.*, **88**, 609 (1990).
38. H.Y. Carr and E.M. Purcell, *Phys. Rev.*, 94, 630 (1954).
39. A. Jerschow and N. Muller, *J. Magn. Reson.*, **125**, 372 (1997).
40. A. Jerschow and N. Muller, *J. Magn. Reson.*, **132**, 13 (1998).
41. J. Lounila, K. Oikarinen, P. Ingman and J. Jokisaari, *J. Magn. Reson.*, **A118**, 50 (1996).
42. H. Nedin and J. Furo, *J. Magn. Reson.*, 131, 126 (1998).
43. M.A. Delsuc and T.E. Malliavin, *Anal. Chem.*, 70, 2146 (1998).
44. L.C.M. Van Gorkom and T.M. Hancewicz, *J. Magn. Reson.*, **130**, 125 (1998).
45. J.K. Nicholson and I.D. Wilson, *Prog. NMR Spectrosc.*, **21**, 449 (1989).
46. M. Liu, X. Mao, C. Ye, J.K Nicholson and J.C. Lindon, *J. Magn. Reson.*, **132**, 125 (1998).
47. D.L. Rabenstein, K.K. Millis and E.J. Strauss, *Anal. Chem.*, **60**, 1380A (1988).
48. W. P. Aue, E. Bartholdi and R.R. Ernst, *J. Chem. Phys.*, **64**, 2229 (1975).
49. A. Bax and D.G. Davis, *J. Magn. Reson.*, **65**, 355 (1985).
50. J.K. Nicholson, P.J.D. Foxall, M. Spraul, R.D. Farrant and J. C. Lindon, *Anal. Chem.*, 67, 793 (1995).
51. M. Ala-Korpela, *Prog. NMR Spectrosc.*, **27**, 475 (1995).
52. M.L. Anthony, B.C. Sweatman, C.R. Beddell, J.C. Lindon and J.K. Nicholson, *Mol. Pharmacol.*, **46**, 199 (1994).
53. E. Holmes, F.W. Bonner, B.C. Sweatman, J.C. Lindon, C.R. Beddell, E. Rahr and J.K. Nicholson, *Mol. Pharmacol.*, **42**, 922 (1992).
54. E. Holmes, P.J.D. Foxall, J.K. Nicholson, G.H. Neild, S.M. Brown, C.R. Beddell, B.C. Sweatman, E. Rahr, J.C. Lindon, M. Spraul and P. Neidig, *Anal. Biochem.*, **220**, 284 (1994).
55. F.Y.K. Ghauri, J.K. Nicholson, B.C. Sweatman, C.R. Beddell and J.C. Lindon, *NMR Biomed.*, 6, 163 (1993).
56. O. Millet and M. Pons, *J. Magn. Reson.*, **131**, 166 (1998).

57. R.D. Farrant, J.C. Lindon and J.K. Nicholson, *NMR Biomed.*, 7, 243 (1994).
58. A.C. Moffat, J.V. Jackson, M.S. Moss and B. Widdop, (Eds) *Clarke's Isolation and Identification of Drugs*. The Pharmaceutical Press, London, 1986.
59. D.J. Birkett and S.B. Wanwimolruk, *Protein Binding Drug Transp. Symp.*, **20**, 1 (1987).
60. X.M. He and D.C. Carter, *Nature* , **358**, 209 (1992).
61. M.C. Meyer and E.E. Gutman, *J. Pharm. Sci.*, **57**, 895 (1968).
62. H.M. Solomon, J.J. Schrogie and D. Williams, *Biochem. Pharmacol.*, **17**, 143 (1968).
63. T.C. Pinkerton and K.A. Koeplinger, *Anal. Chem.*, **62**, 2114 (1990).
64. A. Hersey, R.M. Hyde, D.J. Livingstone and E. Rahr, *J. Pharm. Sci.*, **80**, 333 (1991).
65. C.S. Johnson, Jr., *J. Magn. Reson.*, A**102**, 214 (1993).
66. C. Bertucci, G. Ascoli, G. Uccello-Barretta, L. Di Bari and P. Salvadori, *J. Pharm. Biomed. Anal.*, **13**, 1087 (1995).
67. A.S. Altieri, D.P. Hinton and R.A. Byrd, *Anal. Biochem.*, **229**, 214 (1995).
68. Y. Ma, M. Liu, X.-A. Mao, J.K. Nicholson and J.C. Lindon, *Magn. Reson. Chem.*, in press.
69. Guideline: Test procedures and Acceptance Criteria for New Drug Substances and New Drug Products: Chemical Substances. *International Conference on Harmonisation*, Int. Fed. Pharmaceut. Manufact. Assoc., Geneva, Switzerland, July 1997.
70. N. Mistry, I.M. Ismail, M.S. Smith, J.K. Nicholson and J.C. Lindon, *J. Pharm. Biomed. Anal.*, **16**, 697 (1997).
71. N. Mistry, I.M. Ismail, R.D. Farrant, M. Liu, J.K. Nicholson and J.C. Lindon, *J. Pharm. Biomed. Anal.*, **19**, 511 (1999).
72. J.C. Lindon, *Encyclopedia of Analytical Science*, (Ed.-in-Chief, A. Townshend), Academic Press, London, 1995; p.3408.
73. A. Shaka, J.H. Keeler and R. Freeman, *J. Magn. Reson.*, **53**, 313 (1983).
74. K. Wüthrich, *NMR of Proteins and Nucleic Acids.* 1986, John Wiley, Chichester, UK.
75. S. Grzesiek and A. Bax, *J. Biomol. NMR*, **3**, 627 (1993).
76. C.T.W. Moonen, P. van Gelderen, G.W. Vuister, and P.C.M. van Zijl, *J. Magn. Reson.*, **97**, 419 (1992).

77. A. Böckmann and E. Guittet, *FEBS Letters*, **418**, 127 (1997).
78. M. Andrec and J.H. Prestegard, *J. Biomol. NMR*, 9, 136 (1997).
79. G.E. Hawkes, E.W. Randall, W.E. Hull, D. Gattegno, and F. Conti, *Biochemistry*, **17**, 3986 (1978).
80. C.M. Dobson, L.-Y. Lian, C. Redfield and K.D. Topping *J. Magn. Reson.*, **69**, 201 (1986)
81. M. Liu, H.C. Toms, G.E. Hawkes, J.K. Nicholson and J.C. Linden, *J. Biomol. NMR*, **13**, 25 (1999).
82. M.I. Hrovat and C.G. Wade, *J. Magn. Reson.*, **44**, 62 (1981).
83. B. W. Bycroft, *J. Chem. Soc. Chem. Comm.*, 660 (1972).